AFRL-AFOSR-UK-TR-2019-0023

Short Pulse Mid IR Lasers and Amplifiers via Direct Inscription of Waveguide Devices in ZnSe

Ajoy Kar
HERIOT-WATT UNIVERSITY
RICCARTON
CURRIE, EDINBURGH, EH14 4AS
GB

05/13/2019
Final Report

Air Force Research Laboratory
Air Force Office of Scientific Research
European Office of Aerospace Research and Development
Unit 4515 Box 14, APO AE 09421

REPORT DOCUMENTATION PAGE

Form Approved
OMB No. 0704-0188

1. REPORT DATE *(DD-MM-YYYY)*	2. REPORT TYPE	3. DATES COVERED *(From - To)*
13-05-2019	Final	01 Dec 2016 to 30 Nov 2017

4. TITLE AND SUBTITLE
Short Pulse Mid IR Lasers and Amplifiers via Direct Inscription of Waveguide Devices in ZnSe

5a. CONTRACT NUMBER

5b. GRANT NUMBER
FA9550-16-1-0080

5c. PROGRAM ELEMENT NUMBER
61102F

6. AUTHOR(S)
Ajoy Kar

5d. PROJECT NUMBER

5e. TASK NUMBER

5f. WORK UNIT NUMBER

7. PERFORMING ORGANIZATION NAME(S) AND ADDRESS(ES)
HERIOT-WATT UNIVERSITY
RICCARTON
CURRIE, EDINBURGH, EH14 4AS GB

8. PERFORMING ORGANIZATION REPORT NUMBER

9. SPONSORING/MONITORING AGENCY NAME(S) AND ADDRESS(ES)
EOARD
Unit 4515
APO AE 09421-4515

10. SPONSOR/MONITOR'S ACRONYM(S)
AFRL/AFOSR IOE

11. SPONSOR/MONITOR'S REPORT NUMBER(S)
AFRL-AFOSR-UK-TR-2019-0023

12. DISTRIBUTION/AVAILABILITY STATEMENT
A DISTRIBUTION UNLIMITED: PB Public Release

13. SUPPLEMENTARY NOTES

14. ABSTRACT
Over the past two years a great amount of work has been done in this material resulting in the development of the first CW Ho3+:YAG waveguide laser with both multimode and single mode capabilities. These results were published in Applied Optics in April 2017. Furthermore, the first GHz repetition rate Ho3+:YAG laser ever was demonstrated using a waveguide set-up with graphene as a saturable absorber. The GHz pulses were emitted under a q-switch. These results were presented at CLEO 2017 and so published in the online journal and in turn they have been published in Optics Express in October 2017. The results are promising for modelocking HIP treated CrZnSe for the generation of short pulses. We believe that the choice of saturable will be paramount to doing this and so have 3 a major solutions to try. The first is simply to try a SESAM with better parameters which may be more suitable for this and also to include some dispersion compensation in the cavity. Initially, a new SESAM is going to be used to first establish pulsing ideally in the ps range, and then dispersion compensation to further shorten the pulses will be tried using methods such as; a prism pair, sapphire slab or other appropriate material. We will also attempt to cool the laser crystal and are at present in the process of designing a suitable Peltier cooling system. Another saturable asbsorber we plan to use is Graphene.

15. SUBJECT TERMS
waveguides in Cr+:ZnSe, Ultrafast Laser Inscription, short pulse mid IR sources, EOARD

16. SECURITY CLASSIFICATION OF:			17. LIMITATION OF ABSTRACT	18. NUMBER OF PAGES	19a. NAME OF RESPONSIBLE PERSON
a. REPORT	b. ABSTRACT	c. THIS PAGE			LOCKWOOD, NATHANIEL
Unclassified	Unclassified	Unclassified	SAR		19b. TELEPHONE NUMBER *(Include area code)* 011-44-1895-616005

Standard Form 298 (Rev. 8/98)
Prescribed by ANSI Std. Z39.18

Short Pulse Mid IR Lasers and Amplifiers via Direct Inscription of Waveguide Devices in ZnSe

Final Progress Review

Award Number: FA9550-16-0080

December 2017

F. Thorburn & Ajoy K. Kar*

Institute of Photonics and Quantum Sciences

Heriot-Watt University

Edinburgh

EH14 4AS

Scotland

*Correspondence: a.k.kar@hw.ac.uk

Contents

Introduction

In recent years there has been considerable growth in the demand for sources in the mid-infrared spectral region (2-5 μm). The dramatic growth in this field is due to a lack of available sources which are both robust and compact but which also have high power capabilities and good beam quality[1]. The reason for this is that within this spectral region lies an atmospheric transmission window that overlaps with characteristic absorption lines of a number of molecules; hence there is a vast field of sensing and environmental monitoring applications for mid-IR sources [2]. Other applications of mid-IR sources include medical diagnostic and treatment [3] and military countermeasures [4]. The requirements of a particular source, that is the wavelength, power capabilities, size, running and maintenance costs, are very much dependent on the specific application. For that reason a broad range of different, available sources are required which continuously drives the need for new mid-IR sources [1]. Many applications require pulsed sources with short pulse duration and high pulse repetition frequency, for example high speed optical communication and optical frequency combs for precision metrology. High pulse repetitions are a requirement for these types of applications to obtain the high level of resolution and precision necessary [5-7]. As a result there is a real need to continue the development of new pulsed sources in this spectral range.

Two fields which are currently being explored to develop new mid-IR sources are transition metal doped II-VI semiconductors and Rare Earth doped laser materials. The work done this year has involved both these fields. This report is split into 2 parts. In the first part of the report we will cover the other main topic of our work which is the demonstration of the first Ho:YAG waveguide laser. Both multimode and single mode laser emission was observed and a result the work progressed by using the single mode waveguides to demonstrate a high PRF Q-switched modelocked HoYAG waveguide laser. In part two of this report we will detail the latest progress in the operation of lasers based on Chromium doped Zinc Selenide (Cr:ZnSe) which has been treated using Hot Isostatic Pressing (HIP). This will be explained in greater detail later in this report but this treatment causes the spectral output from a CrZnSe laser to have very narrow linewidth, whereas usually it is much wider for un-treated material. As a result this HIP treated material is an ideal choice for modelocking to generate short ultrashort pulses. The waveguides in this work were fabricated using Ultrafast Laser Inscription.

The work in this report has been done during the past year as part of a long term collaboration between Heriot Watt University (HWU) and the Air Force Research Laboratory (AFRL). The main participants in this collaboration this year have been at HWU; research group leader A. K. Kar and his group members F. Thorburn and A. LAncaster and at AFRL; G. Cook and S. A. McDaniel. This work has been able to progress for another year due to continued funding from EOARD.

Ultrafast Laser Inscription

Ultrafast Laser Inscription (ULI) has become a well-established technique for the fabrication of waveguides in a variety of different materials during the last 15 years and various works have been published detailing the process. Although much of our work is using ULI for waveguide fabrication, we mainly focus on the application of the waveguides in active devices. As a result, only a brief description for the technique shall be given.

The basis of ULI is to tightly focus ultrafast pulses, $\approx 10^{-13}$ s, pulses below the surface of a dielectric material which is transparent to the laser wavelength. This results in a localized permanent change in the material properties at the laser inscription beam focus. The energy transfer processes which occur between the tightly focused ultrashort pulse and the material are very highly complex but I will try to give a summarised version to show how ULI is used in the fabrication of optical waveguides in this work.

The substrate material and ultrafast laser must have appropriate properties to ensure that the photon energy is not great enough to excite electrons from the valence band in the material to the conduction band. Light with energy less than this value would usually experience no absorption as it propagates through the material. However, the use of ultrashort pulses results in high peak powers which create electric fields at the beam focus which is below the surface of the material. These E-fields are great enough to induce nonlinear light-matter interactions; tunnelling and multiphoton ionisation. These in turn result in the creation of a free electron plasma. The laser parameters can be controlled as to confine the plasma to the focus of the laser and the directly surrounding area. Once an electron is excited to the conduction band it can then keep absorbing single photons until it has sufficient energy to ionise another electron which is currently in the valence band. This process is called avalanche ionisation; it repeats as long as the laser irradiates that area, during this process the density of the resulting electron plasma exponentially increases. The laser will resonantly drive plasma oscillation when the plasma density is such that its resulting frequency matches that of the laser radiation. At this point a significant portion of an incident pulse will be absorbed and as the pulse leaves the focus of the beam the plasma transfers energy to the relatively cold surrounding lattice. The heating of the lattice by the plasma is very efficient as thermal diffusion is kept as low as possible. Due to this only the material that has been in the laser beam focus and the directly surrounding area is affected. This heating process can cause the material to melt or change to another phase, gas or plasma, and as the heat leaves the material solidifies with a permanently altered structure. There are a number of ways in which the material can be modified, for example a change in refractive index or chemical etch rate.

Other waveguide fabrication methods such as lithography require clean room environments and fabrication time can be lengthy - which can make them impractical techniques. The primary advantage of ULI over these other methods is that it does not require a clean room and multiscan waveguides can be fabricated very quickly i.e. on a minute time scale. In addition, lithography methods result in 2D waveguides on the medium surface which are very susceptible to damage, a cap is often used for protection but this is often expensive. The type of 3D waveguides that ULI produces require no such protection as they are buried beneath

the material surface. The primary disadvantage of using waveguides inscribed by ULI for a waveguide laser application is that the losses which occur during the total internal reflection at waveguide boundaries (propagation loss) can be significantly higher than the free space propagation losses through bulk media. This must be accounted for to ensure the total gains exceed the losses.

For the fabrication of waveguides we can use the change in refractive index; this can happen if the laser is used in a regime where the pulse energy is slightly larger than the material modification threshold. If the material is translated with nm precision through the laser beam focus, a region of material with modified refractive index can be produced, this is demonstrated in Figure 1. The index change can be positive or negative. The ULI parameters – power, translation speed and the NA of the focusing lens, as well as the particular material properties determine the type of modification which occurs and we can control the parameters to select the specific type of waveguide inscribed. There are 3 types of waveguide that can be inscribed and these are shown schematically in Figure 2.

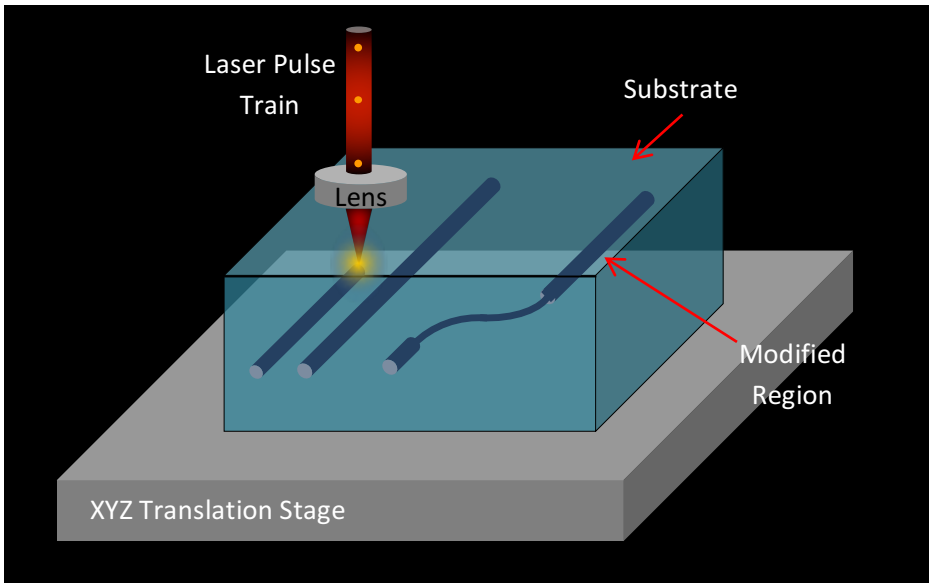

Figure 1. Diagram which demonstrates how the sample is translated through the pulsed laser focus using high precision translation stages resulting in tracks of modified material.

As shown in Figure 2a., a type 1 waveguide is the result of a net increase in the material index and so light can be guided along the modified region. Type 2 waveguides, see Figure 2b., are produced by inscribing 2 parallel lines of catastrophic damage; in this case guiding is made possible through an index change which is a result of the stress-optic effect induced by the damage lines. The light will be guided between the 2 inscribed lines. The last type are demonstrated in Figure 2c. and are called depressed cladding structures. A net decrease in the material index is used to inscribe a series of lines which result in a modified cladding region and the light can be guided in the internal unmodified region. The ULI method can be used to

inscribe waveguides in a variety of materials including glasses and photonic crystal structures.

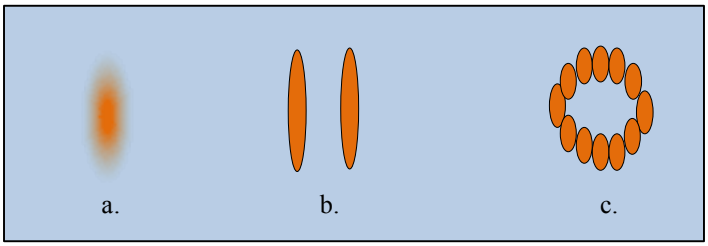

Figure 2. Diagram depicting the 3 types of ULI waveguide. a. Type I, b. Type II, c. Depressed Cladding structures.

In glass materials Type 1 structures can be easily produced and generally these waveguides generally exhibit lower propagation losses than type 2 or depressed cladding waveguide structures. However, the depressed cladding waveguide seems to be the preferred waveguide type for devices in the mid-IR, this is because this method allows more control over the waveguide cross sections which is very important when compared to the other types. The ULI method can be used to inscribe waveguides in a variety of materials including glasses and photonic crystal structures [8-13].

At HWU ULI of waveguides is performed using the IMRA uJewel D400, this is a chirped pulse amplifier, fibre MOPA (Master Oscillator Power Amplifier). The system allows the user computer control over the laser power and polarisation. In addition, the user controls translation of the sample substrate through the laser beam with nanometer precision using XYZ (Aerotech) air bearing stages. The inscription system arrangement is shown in the Figure 3. The AOM (acousto-optic modulator) is included in the apparatus to allow rapid modulation of the inscription beam for the fabrication of periodic features such as Bragg gratings.

a)

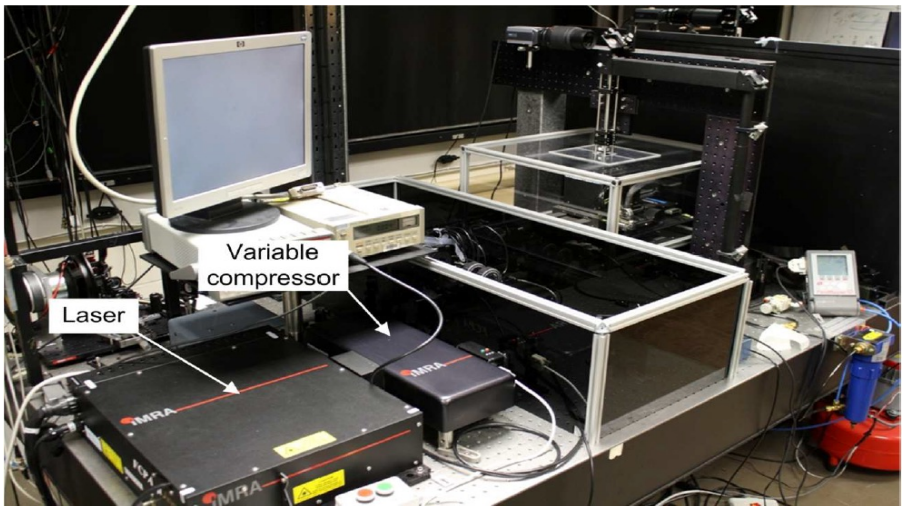

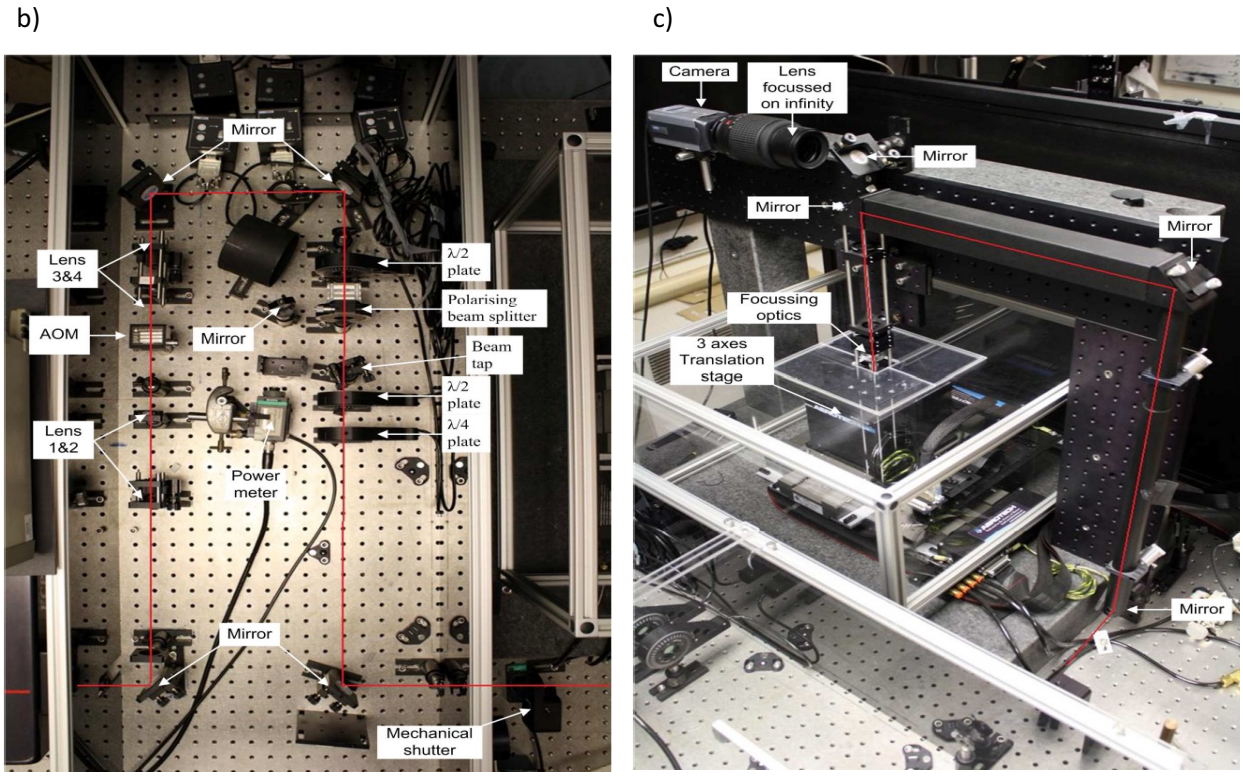

Figure 3. Ultrafast laser inscription apparatus: a) IMRA inscription laser and variable compressor. b) Power and polarisation control. c) IMRA inscription laser beam path, focusing optics and imaging system.

Holmium doped YAG Waveguide Laser

Holmium doped Yttrium Aluminium Garnet (Ho^{3+}:YAG) is a very well established laser gain medium which is most commonly pumped at 1.9 µm and used as a source for emission at approximately 2.1 µm [14-17]. YAG itself is a very useful host crystal in the fabrication of solid state laser materials because it is readily acceptant of both Rare Earth and Transition metal dopant ions – as a result, it has been used to develop a wide range of lasers in the visible, infrared and mid-infrared [18]. Nd^{3+}:YAG can be used to emit at a number of visible and infrared wavelengths but 1064 nm is the most commonly used emission band [19]. Other examples include Yb:YAG which is used for 1030 nm lasers [20], Chromium doped YAG for emission ~ 1.32-1.53 µm [21] and Er^{3+}:YAG which is used for its emission at ~ 2.9 µm [22], and also 1.6 µm [23]. Ho^{3+}:YAG and Tm:YAG [24] materials are used for their emission around 2 µm. As our work is concentrated on developing lasers in the 2-5 µm range Ho doped YAG is of particular interest and a laser at this wavelength could potentially be a useful source for the pumping of CrZnSe lasers which is one of the main focuses of our work. The first HoYAG lasers emitting at 2.1 um were co-doped to optimise the absorption of pump light. The codopants used were Er [25], Cr [26], and most often Thulium resulting in a pump wavelength of ~ 800 nm, this became the most common co-dopant after the development of high power diodes at this wavelength [27-29]. However, the primary way to use singly doped

HoYAG crystal is to in-band pump at 1.9 µm. This pumping scheme is shown in Figure 4. and it relies on Stark Splitting occurring to result in the required population inversion for laser emission at 2.1 µm.

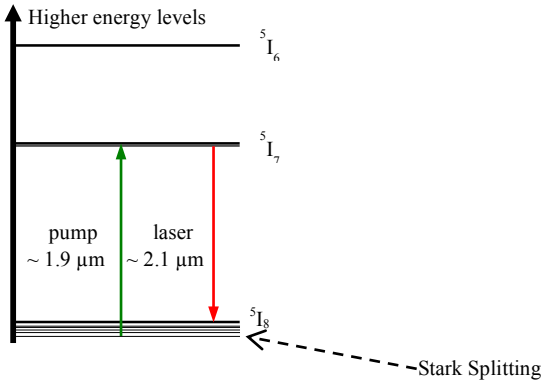

Figure 4. Energy level diagram for Ho^{3+}:YAG crystal.

The advantage of using this in-band pumping scheme is that the 1.9 µm sources required for pumping are widely commercially available, specifically, in the form of Thulium doped fibre lasers which can have high power capabilities and good beam quality [15-17]. Much of the work done in HoYAG lasers has been in bulk and has required the use of cryogenic cooling the material to around 77 K in an attempt to reduce the detrimental thermal effects common to the material [14]. These effects include a low thermal conductivity (~ 11 $Wm^{-1}K^{-1}$ at room temperature [30]) which means that dissipation of heat within the material is not efficient, leading to limited CW laser performance and the ceasing of lasing altogether at high pump powers. In addition to this, HoYAG bulk lasers tend to exhibit high laser thresholds due to a relatively low absorption cross section at the pump wavelength but cooling the material reduces the population of the lower laser level and hence reduces the laser threshold compared to at higher temperature [14]. The large size of bulk CW HoYAG lasers (metre scale), as well as equipment required for efficient cooling, can mean that they are unsuitable for many applications where the space/money required is simply not available. An Ultrafast Laser Inscription fabricated waveguide laser can provide a solution to the thermal issues presented in bulk HoYAG. This is because a waveguide ensures good overlap between pump and signal beams which can lower the laser threshold significantly and higher efficiency in the conversion of pump to signal energy so that the high pump powers which can cause these thermal issues may not be required. The gain in a waveguide laser can be very high per unit length compared to bulk systems if the ideal inscription parameters are identified, so they can be made on a much smaller (mm) scale. The work we did last year resulted in the first demonstration of a CW HoYAG waveguide laser in this material and this year in April the results were published in Applied Optics [31]. Depressed cladding structures were inscribed for this work as these tend to be much better for the propagation of mid-IR wavelengths compared to the other two waveguide types. This is because when scaling the waveguides up for propagation at these wavelengths the crystals tend to crack if a Type I inscription is attempted. Furthermore, the cladding structures are lower loss than Type II. As ULI has already been used successfully to fabricate depressed cladding waveguide lasers in Tm:YAG

[32] and Nd:YAG [33], it was sensible to use them in Ho:YAG as well. Last year we also began working towards a pulsed HoYAG waveguide laser and the initial results were detailed in last years report. During the course of this year this work was continued and the full results of a Q-switched modelocked HoYAG waveguide laser will now be given.

Q-Switched Modelocked Waveguide Laser

We report a ~ 2.1 μm monolithic waveguide laser operating in a Q-switched modelocked (QML) regime with a high pulse repetition frequency (PRF) of 5.9 GHz. The laser is passively modelocked using a film of a number of graphene layers coated onto an output coupler. This is the first demonstration of GHz pulses emitted from a Ho^{3+}:YAG laser.

Despite over 2 decades of research into and use of Ho^{3+}YAG lasers there have been few demonstrations of singly doped HoYAG modelocked lasers with short pulse widths and none until this work with a GHz PRF. Only very recently was the first femtosecond demonstration of a Ho^{3+}YAG laser which has a very impressive pulse length of 220 fs [34]. Until this, the shortest pulse length demonstrated was 2.1 ps which operated with a PRF of 82 MHz [35]. As stated, the laser we have demonstrated emits QML pulses. This is when a laser outputs passively modelocked pulses under the envelope of a q-switch [36]. As a result of this behaviour, there is the potential for a great amount of energy to be stored within the q-switch and so very high peak powers are possible – much higher than could be achieved with a CW modelocked set-up. Whilst for many applications QML is not suitable, the advantage of it is that it is ideal for use as a source for subsequent amplification. The delay between groups of pulses emitted during QML can allow appreciable energy storage in amplifiers, leading to very high power pulse generation. Conversely, pure CW mode locking often requires "pulse pickers" to isolate single pulses or groups of pulses in order to realize appreciable energy gain in later amplifier stages.
Depressed cladding structures, detailed in the Ultrafast Laser Inscription sections were inscribed into a substrate of 0.5%Ho:YAG with dimensions 5×5×14 mm. The waveguides were written in the long length of the sample. The waveguide which was found to have optimum efficiency and single mode operation was 50 μm in diameter and made up of 60 individual inscription elements. The input facet of this waveguide is shown in Figure 5.

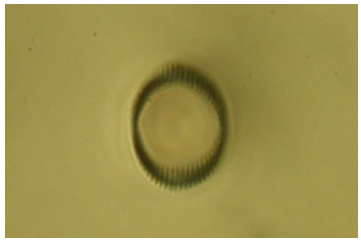

Figure 5. End facet of depressed cladding waveguide structure inscribed in Ho^{3+}:YAG substrate

The inscription laser used, which is pictured in the ULI section, operated with a pulse repetition frequency of 500 kHz, pulse duration of ~ 360 fs and a central wavelength of 1043 nm. The laser pulses were focused at a distance of 250 μm below the surface of the HoYAG

substrate by a 0.4 NA lens with a focal length of 6.2 mm, resulting in a focal spot of 2 μm. Each element was inscribed at a speed of 10 mm/s and an average laser power of 125 m, consequently the pulse energy was 250 nJ. A full CW laser characterisation on this waveguide was part of the work done last year and can be found in the paper [31] which was published this year.

The Saturable Absorber (SA) which was chosen to produce pulsed operation was a Graphene coated (standard reflective) output coupler (GSOC). Graphene has attracted much attention as a saturable absorber (SA) in the development of ultrafast pulsed laser sources. This is because this material has intrinsic broadband operation, low saturation fluence and ultrafast recovery time [37]. In addition to these parameters, a single layer/multiple layers of graphene can be coated with some ease onto a standard reflective output coupler resulting in a Graphene coated Saturable Output Coupler (GSOC) which can be a useful alternative to more common SA's such as Semiconductor Saturable Absorber Mirrors (SESAMs) which have complex fabrication procedures [38].The output coupler was 80% reflective from 1.7 – 2.7 μm resulting in a double pass of the 1.9 μm pump signal. The graphene coating process was carried out by transfer from commercially available graphene coated copper foil and a detailed explanation of this can be found in [39]. The result is that the output coupler is coated with a few layers of Graphene, typically < 10, at any given point on the surface. After coating, a nonlinear transmission measurement was carried out to give us an idea of the saturable absorption properties of the GSOC. This was done using an optical parametric amplifier tuned to 2.1 μm which generated 100 fs pulses at a rate of 1000 Hz. The GSOC was positioned in the path of the OPA beam and a measurement of the transmitted output power was made as a function of the input pulse fluence, where fluence is the optical energy per unit area. This result is shown in Figure 6.

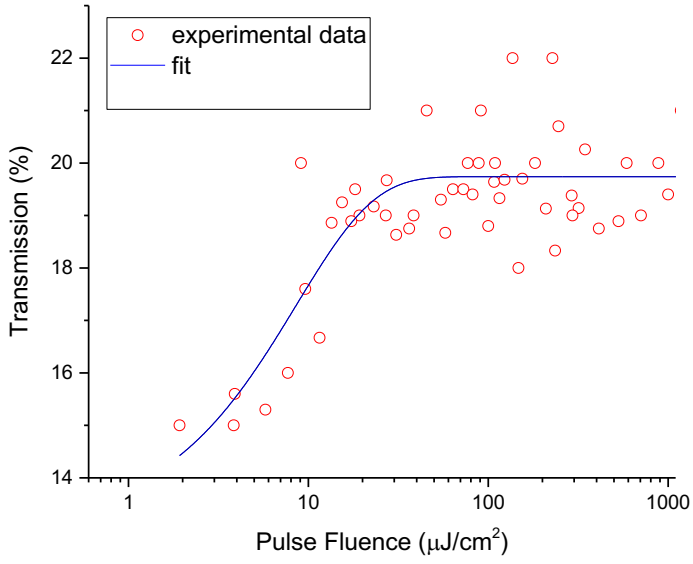

Figure 6. Nonlinear transmission versus pulse fluence for GSOC.

This result renders the GSOC to have a saturation fluence of 8.6 µJ/cm^2, a modulation depth of 6.6 % and the nonsaturable loss is 80.3%.

The Laser cavity was set-up as shown in Figure 7.

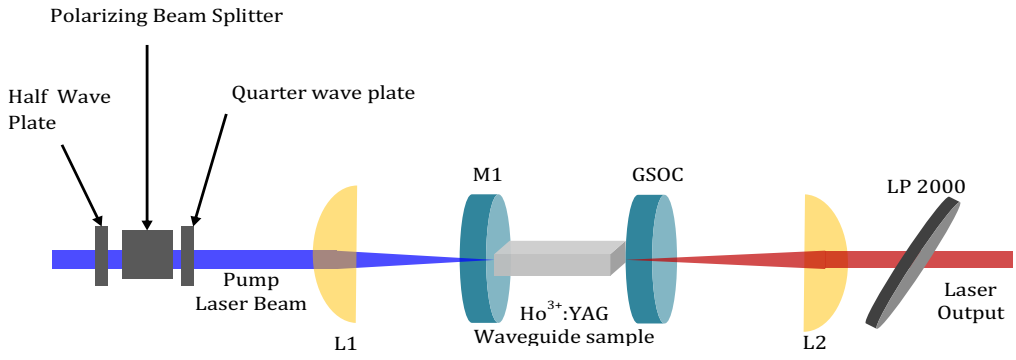

Figure 7. Cavity configuration for QML HoYAG waveguide laser.

The pump source used was a CW, linearly polarised, Tm doped fibre laser emitting at 1908 nm (IPG mode TLR-1908-LP), with a maximum output power of 12 W. The polarising beam splitter and wave plate alignment in the path of the incident pump beam is there to protect the pump laser from any feedback into the laser from Fresnel reflections at interfaces in the set-up, the result is a circularly polarised pump beam. L1 is a plano-convex lens used to focus pump light into the waveguide, it has a 40 mm focal length which was found to produce optimum coupling into the 50 µm waveguide. L2 is a 50 mm focal length plano-convex lens for collimating the output. Both lens are antireflective (AR) coated from 1.65 to 3 µm. M1 is the cavity pump mirror which is AR coated on the rear side to allow pump light to pass and HR coated on the front side for 2.05-2.43 µm. As discussed previously the GSOC is 80% reflective at the laser wavelength. The LP 2000 filter directs any unabsorbed pump power into a beam dump before measurements are made on the output laser beam. Careful alignment of the laser cavity and specifically M1 and the GSOC resulted in pulsed laser operation at ~ 2.1 µm. The optimum Q-switched mode-locking results obtained are displayed in Fig. 8.

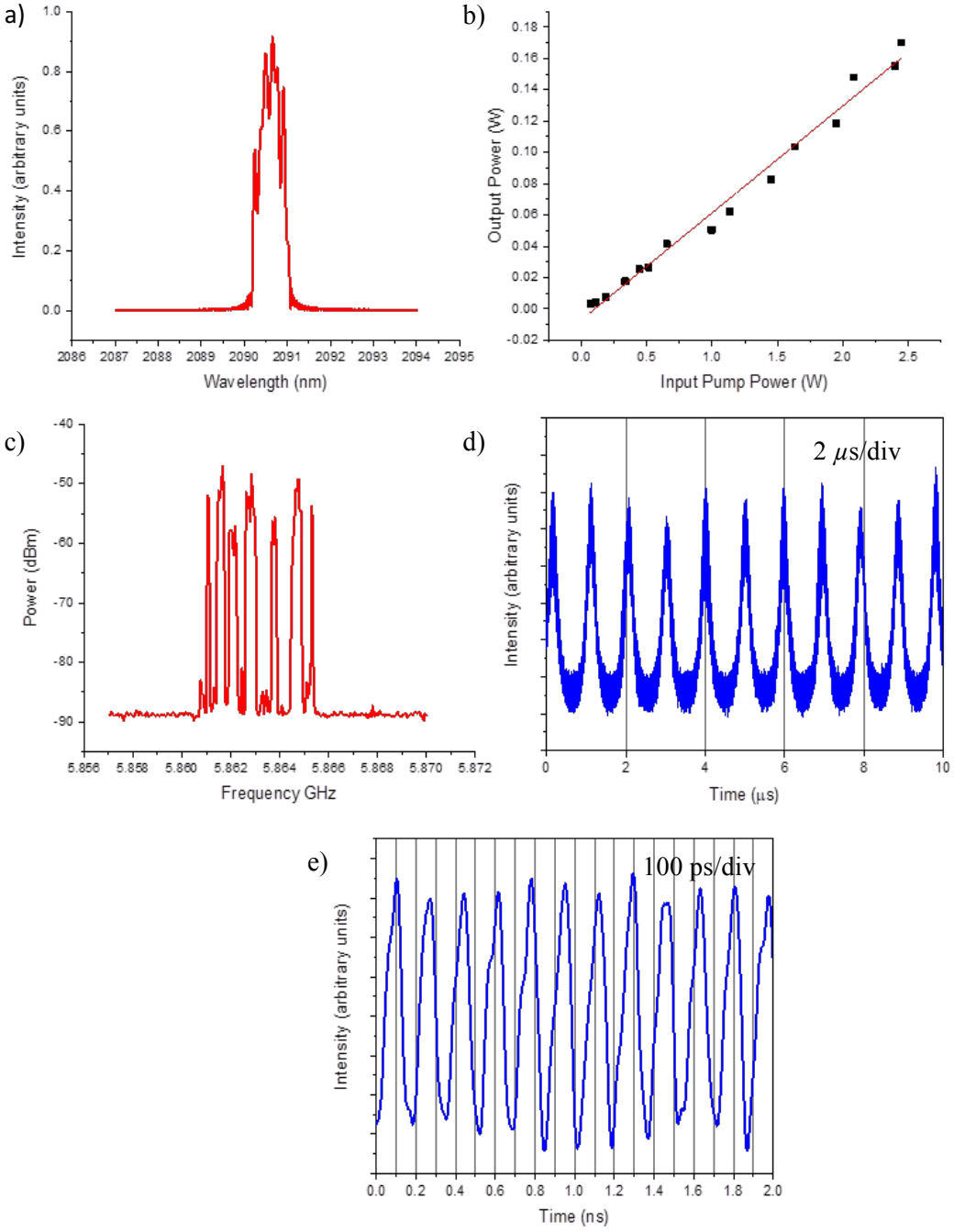

Figure 8(a) QML waveguide laser spectral output, (b) output power vs. incident pump power, (c) RF spectrum: this graph has a span of 150 MHz and was taken with a res. bandwidth of 1 kHz, (d) q-switched pulse train, (e) modelocked pulse train.

A Thorlabs Optical Spectrum Analyser (OSA205) hown in Fig 8(a). The spectrum is centred at 2091 nm and has a bandwidth with FWHM of ~ 0.8 nm. The graph in 8(b) shows the output power as a function of incident pump power giving a slope efficiency of 6.8%, the maximum output power obtained was 170 mW at an incident power of 2.5 W. Damage to the surface of the graphene was observed at a pump power = 2.7 W and so the damage threshold of the GSOC was estimated to be ~ 1.6 μJ/cm^2. As a result the pump power used in the experiment was restricted to a maximum of 2.5 W to ensure the Graphene would not be

damaged. The laser was found to be QML on the onset of threshold and no q-switching only region was observed, this is likely due to the saturation characteristics of the Graphene layer.

The RF spectrum of the laser output is shown in Fig 8(c), this was measured using a 13 GHz RF spectrum analyser (Agilent E4405B ESA-E) along with a high speed 12.5 GHz InGaAs photodetector (Newport 818-BB-50). This shows us that the pulses being emitted under the q-switch are doing so with a PRF of 5.860-5.865 GHz. There are a number of peaks in the spectrum as opposed to the 1 single narrow peak which would be expected for a CW modelocked output and this is the first implication the that the laser QML. This was confirmed by viewing both the q-switch and the modelocked pulses using a 23 GHz Tektronix MSO/DPO72304 oscilloscope connected to the high speed detector previously described, these results are shown in Figs 8(d) and (e) respectively. The q-switches are emitted with a repetition rate of 1.04 MHz resulting in a pulse energy of 0.16 μJ per q-switch envelope. The PRF of the modelocked pulses can be estimated theoretically using:

$$f_{rep} = \frac{c}{2nl} \tag{1}$$

In equation 1 c [ms^{-1}] is the speed of light, n is the refractive index in the cavity and l is the cavity length [40]. In this case the result is an estimated PRF of 5.9 GHz which is in good agreement with the results shown in Fig 8(c). We found that this QML behaviour was very stable for several hours at low pump powers but when increased to values > 2 W after some time the laser exhibited rapidly changing peak power and sometimes stopped pulsing altogether. This is likely due to both thermal issues in the cavity as heat builds up over time and possible damage to the graphene after long exposure to higher powers.

There exists a stability criterion by which we can verify the q-switched modelocked behaviour exhibited by the laser and this is shown in Eq. (2) in which the critical pulse energy $E_{P,c}$ is calculated. The critical pulse energy is defined as the minimum pulse energy required to escape the region of q-switching instabilities and so operate purely in the CW modelocked regime. As a result, at pulse energies less than $E_{P,c}$ the laser operates in the QML or only q-switched regime.

$$E_{P,c} = \left(E_{sat,L} E_{sat,A} \Delta R\right)^{1/2} \tag{2}$$

In this equation, $E_{sat,L}$ is the saturation energy of the laser gain material (Ho^{3+}:YAG), this is the produsct of the effective laser mode area inside the material itself and the inherent material saturation fluence. Similarly, $E_{sat,A}$ is the same parameter for the saturable absorber which in this case is the GSOC, it is the product of the saturation fluence of the Graphene film and the effective laser mode area incident on it. ΔR is the modulation depth of the GSOC which was measured previously as 6.6% (see above) [36]. These are all known/calculated parameters and so when inserted into the equation, $E_{P,c}$ is calculated to be $\approx 2.6\times10^{-8}\,J$. The maximum intracavity pulse energy emitted by the laser is found to be $E_P \approx 2.9\times10^{-11}\,J$, this is 3 orders of magnitude less than the critical pulse energy and so is in good agreement with experimental results and verifies that the laser is operating well within the QML instabilities limit. Although QML can be advantageous for some applications as discussed

previously, in many cases it is not desirable and a stable CW mode-locked source is required. To get this laser to this stage there are some adjustments which could be made including; the GSCO should have a higher reflectivity value to increase the intracavity energy, as well a smaller modulation depth. Also, a lower loss waveguide would lead to an increase in the slope efficiency and therefore the maximum output power could be improved. This, alongside the careful design of the GSCO parameters could result in a cavity which is optimized to operate with a stable CW modelocked output whilst sustaining the high PRF due to the short length of the cavity. The initial results from this work were presented at CLEO 2017 [41] and then in turn the full results published in Optics Express [42].

Future Work

The future work using this material will focus on demonstrating CW mode-locked operation from a single mode ULI waveguide. Work has begun on setting up a cavity which will use a SESAM as the SA but this does complicate the cavity a little. A schematic of this set-up is shown in Figure 9.

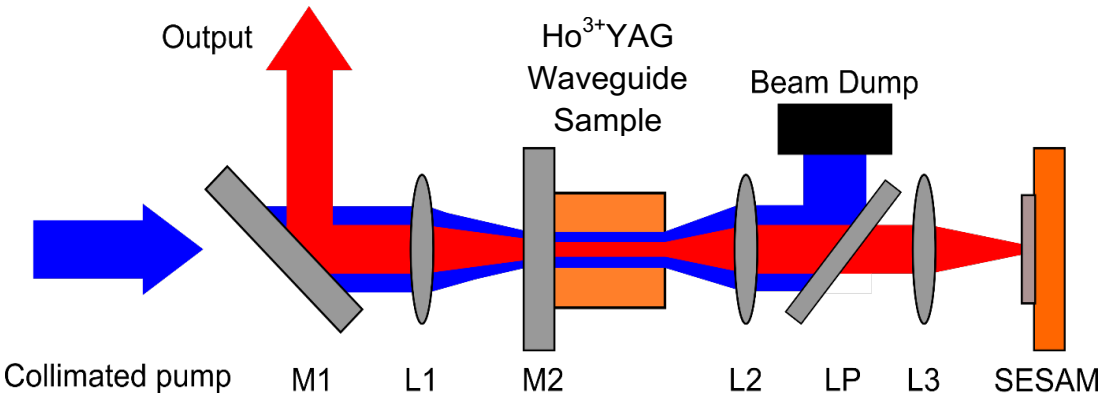

Figure 9. Schematic of Modelocked Ho^{3+}YAG waveguide laser using SESAM. M1 is a 45º degree dichroic mirror AR coated for 1.9 µm on rear and HR for 2.1 µm on front, M2 has same coatings for 0º incidence angle. L1, L2 and L3 are 50 mm plano-convex CaF_2 lenses which are AR coated 1.65-3 µm. LP is a 2000 nm long pass filter which is used to direct any unabsorbed pump light into a Beam Dump to protect the SESAM from damage.

The SESAM available to us is a commercial BATOP SAM which is ~ 98.5 reflective at 2.1 µm, has a saturation fluence of 70µJ/cm^2, a modulation depth of 1.2% and a relaxation time constant of ~ 10 ps. The aim is to fabricate a single mode waveguide which when used in this cavity results in stable CW modelocked output, initially the cavity length will be longer (~ 0.5 m) but this will be reduced after initial demonstration in an attempt to maximise the PRF. Another method to obtain this would be to fabricate a new GSOC carefully designed to increase the intracavity energy and reduce the modulation depth levels which will overcome the q-switching instabilities, we are in contact with other groups to see if this design will be possible.

Summary

Over the past two years a great amount of work has been done in this material resulting in the development of the first CW Ho^{3+}:YAG waveguide laser with both multimode and single mode capabilities. These results were published in Applied Optics in April 2017. Furthermore, the first GHz repetition rate Ho^{3+}:YAG laser ever was demonstrated using a waveguide set-up with graphene as a saturable absorber. The GHz pulses were emitted under a q-switch. These results were presented at CLEO 2017 and so published in the online journal and in turn they have been published in Optics Express in October 2017.

Chromium doped ZnSe Lasers

There has been a great deal of work done in the development of CrZnSe waveguide lasers since the start of this collaboration. I will first give a very brief summary of the work carried out previous to this year and then I will detail the results of modelocking experiments with particular focus on how the Hot Isostatic Pressing treatment of CrZnSe has become forefront to this.

Initial work on the project saw the fabrication of low loss depressed cladding waveguide structures in Chromium doped Zinc Selenide. The result of this was the first demonstration of a ULI CrZnSe waveguide laser which had a slope efficiency of 45% and an output power of 285 mW [43]. Power scaling of this set-up led to a large increase in the maximum output power to 5.1 W with a threshold of 350 mW and slope efficiency of 41 % [44]. Modelling of the thermal limitations of the waveguides was carried out and gave indications of how to improve this further. A tunable waveguide laser was also demonstrated using a Si prism and a rotation mounted output coupler, it demonstrated a tunable range of 803 nm, the widest ever achieved from a waveguide laser [45]. However, the focus of our results were taking the transverse single mode waveguides and attempting to modelock for the generation of ultrashort pulses.

In 2016 a modelocked CrZnSe waveguide laser was demonstrated using the cavity shown in Figure 10.

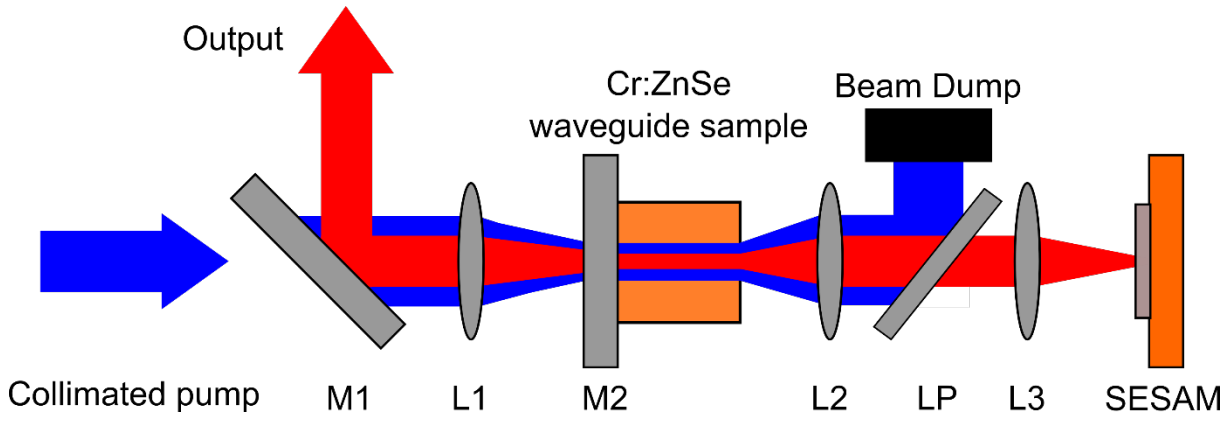

Figure 10. Schematic of modelocked Cr:ZnSe waveguide laser set-up. M1 is a 45º dichroic which is AR coated for the pump and Highly reflective from 2-3 µm. M2 is AR coated for the pump and 98% reflective for 2-3 µm. L1 and L2 are 50 mm plano-convex lenses for focusing into the waveguide and collimating the output beam. LP is a 2000 nm long pass filter to protect the SESAM from damage due to any unabsorbed pump light.

The SESAM used (Del Mar Photonics SAM-2400-1-25) has a saturation fluence, time constant and modulation depth of 90 µJ/cm^2, 500 fs and 0.6% at 2400 nm respectively. This cavity resulted in a stable CW modelocked output. The laser was investigated at 3 different cavity lengths to explore what effect increasing the PRF had on the pulse length. At a PRF of 308 MHz the laser was found have an average output power of 85 mW when pumped with a maximum of 5 W and a pulse width of 638 fs assuming a sech^2 pulse. By reducing the cavity length to 15.6 cm the PRF increases to 961 MHz, the average output power for 5 W of pump power is 68 mW and the pulse length is 1477 fs. The cavity length was further reduced by 1 cm resulting in a PRF of 1.03 GHz, average output power of 74 mW and pulse width of 2024 fs. However, on further investigation of the autocorrelations obtained it was found that the peak to wings ratio was 4:1, whereas in a stable CW modelocked laser we would expect this to be 8:1. In addition the autocorrelation for in particular the shortest cavity length was found to have an underlying beat, this is shown in Figure 11 (d).

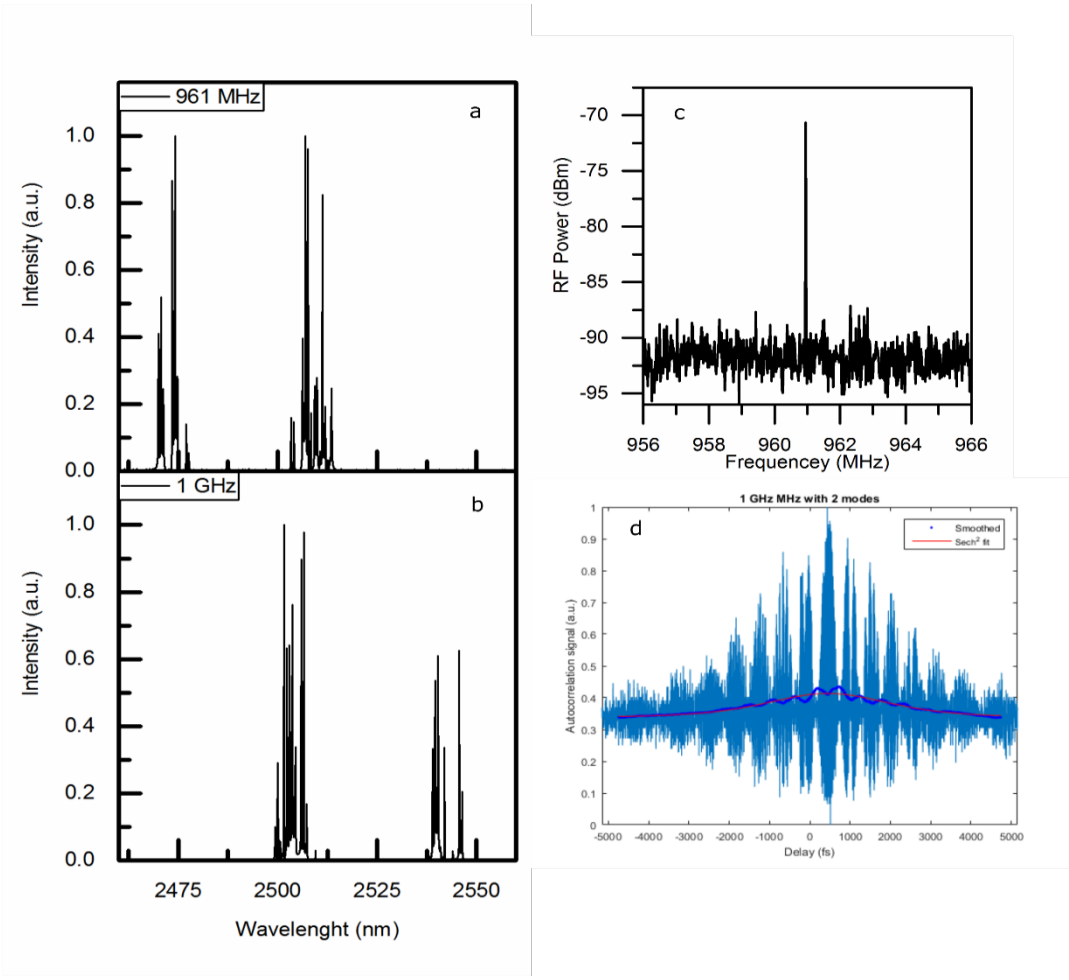

Fig. 11. a) Wavelength spectra of laser with PRF of 961 MHz and b) 1.03 GHz. c) RF spectrum at PRF = 961 MHz. d) autocorrelation for PRF = 1.03 GHz.

We think that this is due to interaction of 2 longitudinal modes within the cavity, as we can see in Fig. 11(b), there are many lines of emission in the output spectrum. Multiple emission peaks means it can be very difficult to modelock as locking the phase between so many modes is very difficult. One possible solution to this is to use laser material which has been treated using Hot Isostatic Pressing. AFRL have carried out a great deal of work using HIP in a new technique for the post growth diffusion of transition metal doped II-VI materials. This new technique has shown to result in a much faster diffusion process than in more traditional methods. One of the effects of this is that the treated materials free running spectral bandwidth is reduced by many orders of magnitude compared to materials which are doped with other methods not using this HIP treatment. A detailed explanation and further information about the process of HIP treating transition metal doped materials can be found in [46] but I will not go into much more detail here as the work in developing this technique was all carried out at the AFRL. In this paper the authors demonstrate this effect by presenting results from a bulk CrZnSe laser in which the crystal has had this treatment. The spectral linewidth is 140 pm and is limited by the resolution of the Thorlabs OSA used to test it. A commercially available piece of CrZnSe laser crystal results in a linewidth which can span many 10ns of nm. This dramatic reduction in the spectral width makes this HIP treated material an ideal candidate for modelocking studies, by reducing the number of emission

peaks and so number of wavelengths emitted, there as a much high chance that the different modes are able to be locked in phase with each other. I will now present and discuss the results that have been obtained this year using this new material.

HIP treated CrZnSe Laser

Our initial goal was to use the HIP treated material to fabricate a CW modelocked, high repetition rate CrZnSe waveguide laser with a short, fs, pulse width. However, during initial inscription investigations at the AFRL it was found that the heat treatment largely effects the ability to inscribe waveguides in the same was as done previously. As a result we first carried out some bulk lasing experiments as well as testing the waveguides. A schematic of the cavity used to do the bulk investigation is shown in Fig. 12.

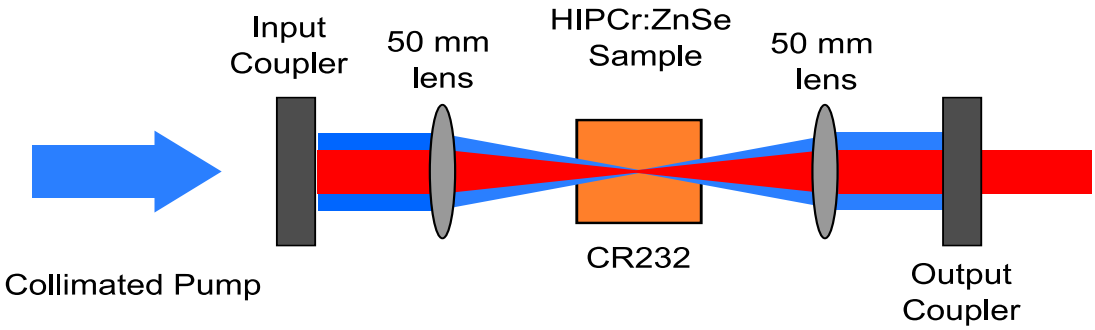

Figure 12. Diagram of bulk plane-plane HIP CrZnSe laser set-up. CR232 is the sample identification number.

The power performance for 70% and 80% reflective output couplers is shown in Figure 13. The spectral output of this cavity was measured with a Thorlabs OSA with 0.1 nm resolution and is shown in Figure 14.

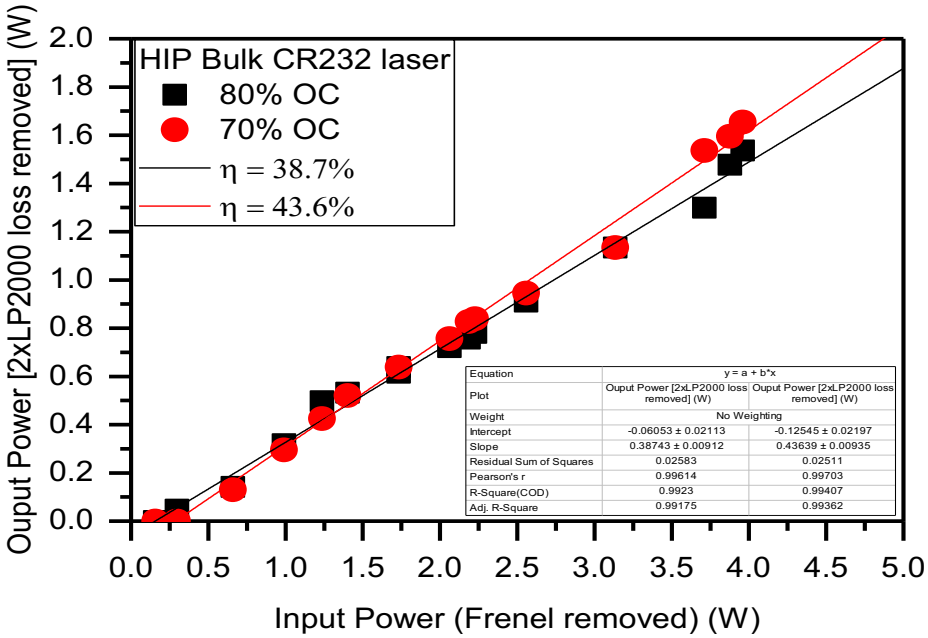

Figure 13. Power performance of HIP CrZnSe bulk plane-plane cavity.

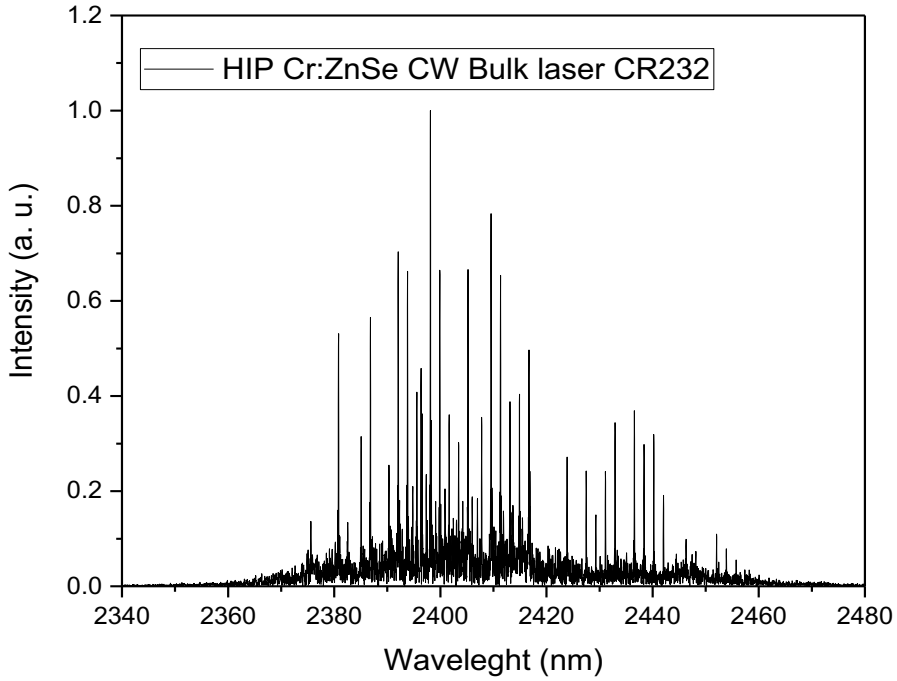

Figure 14. Spectral Emission from HIP CrZnSe bulk plane-plane cavity.

The result in Fig. 14. is unexpected as with the HIP treatment we would expect a single narrow peak. At this stage the polarisation of the pump light was changed from circular to linear and this result is shown in Figure 15.

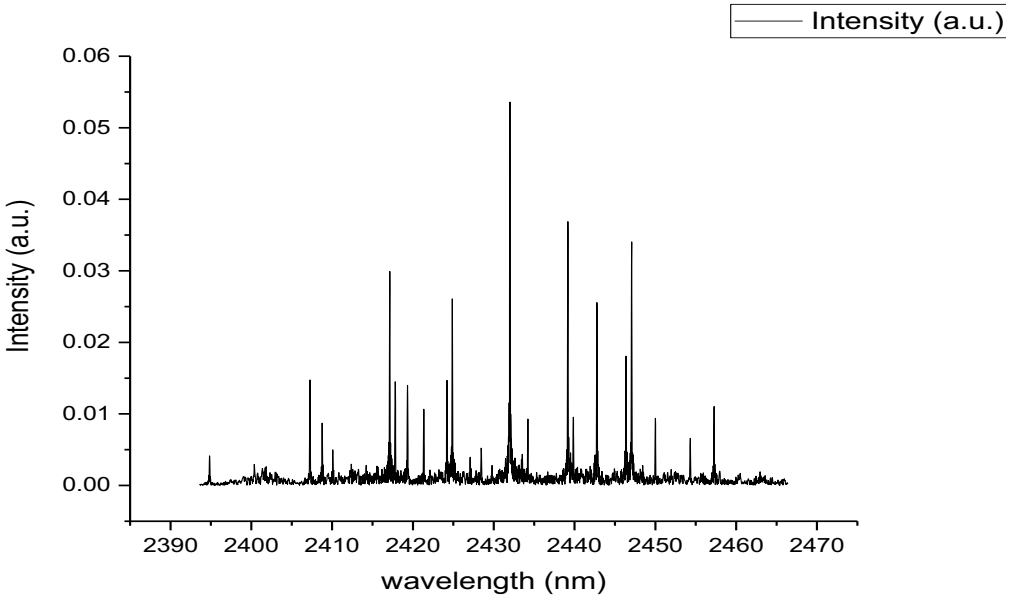

Figure 15. Spectral emission from HIP CrZnSe bulk laser with linearly polarised pump light.

Clearly there are still an unexpected number of emission peaks in the output. After discussions between HWU and AFRL it was decided that the sample must be aligned at Brewster's angle to emit only the one narrow peak as desired. In addition to this, investigations into the performance of ULI waveguides in another sample of HIP treated CrZnSe (sample CR224) were carried out. It was found that the inscribed waveguides had high loss compared to waveguides used in previous untreated CrZnSe studies and as a result the output power was limited to a maximum of 0.5 W for a pump power of 5 W, this result was taken from the optimum waveguide we could identify. A mode profile and spectral emission from this waveguide are shown in Figure 16 (a) and (b) respectively.

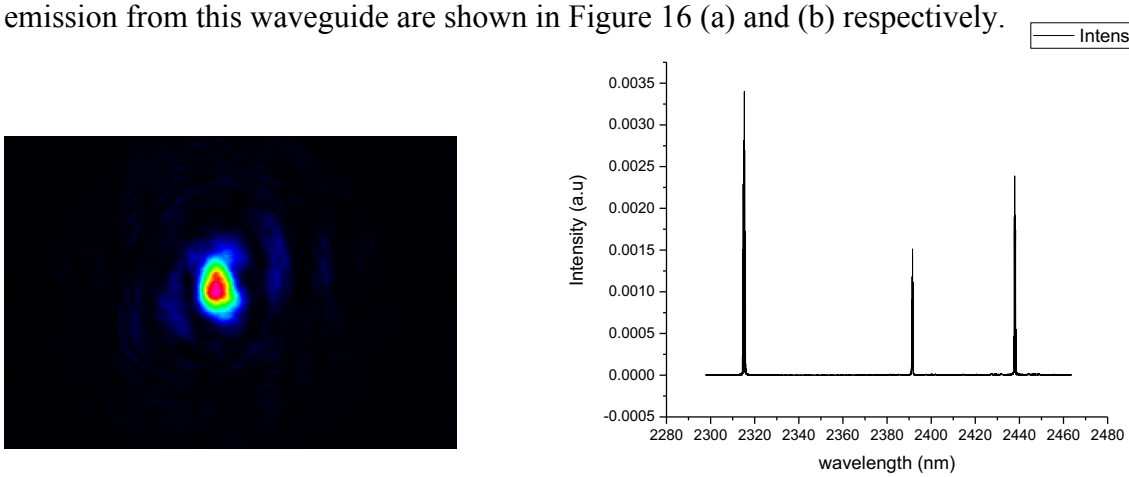

Figure 16 a) Laser mode profile from waveguide laser. b) Spectral emission from waveguide laser.

From these results we can see that waveguide is highly lossy as there seems to be some strain guiding in the inscription region. There are 3 emission peaks in the spectral output from the waveguide laser. This is not a good result and it seems that the inscription process is having adverse effects on the treated material, investigations into this are ongoing at the AFRL. At

this stage it was decided that the next sensible to take would be to build a Brewster angle bulk cavity at HWU and first attempt to modelock the new material this way initially.

HIP treated CrZnSe Bulk Z-cavity Laser

The cavity shown in Figure 17 was built at HWU using the bulk area in sample CR224.

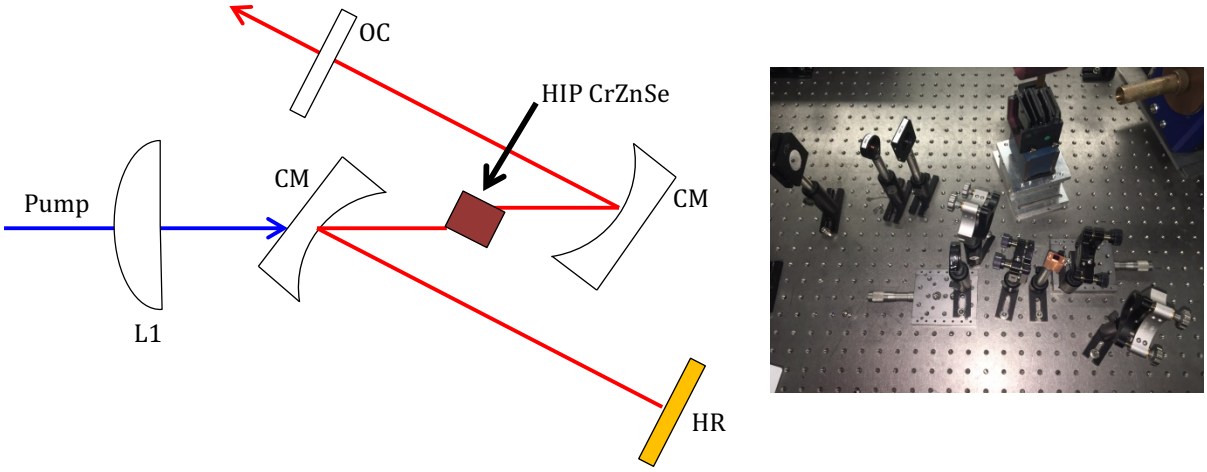

Figure 17. Z cavity set-up. The HIP CrZnSe sample is orientated at Brewster's angle between 2 curved mirrors (CM) which have ROC = 50 mm. These mirrors collimate the beam between the first CM and HR, this is a highly reflective (~99%) plane mirror and between the second CM and the OC – output coupler. L1 is a lens which mode matches the pump to the resonator.

The output coupler used in this CW investigation is a plane mirror which is 80% reflective from 1.7 – 2.7 µm. The laser is pumped with a 20W 1.9 µm Tm:fibre IPG laser which is fully described in the QML HoYAG laser section. The polarisation orientation of the pump is in the plane of incidence so that all the pump light is transmitted through the crystal. The laser results from the HIP treated CrZnSe in this cavity are shown in Figure 18.

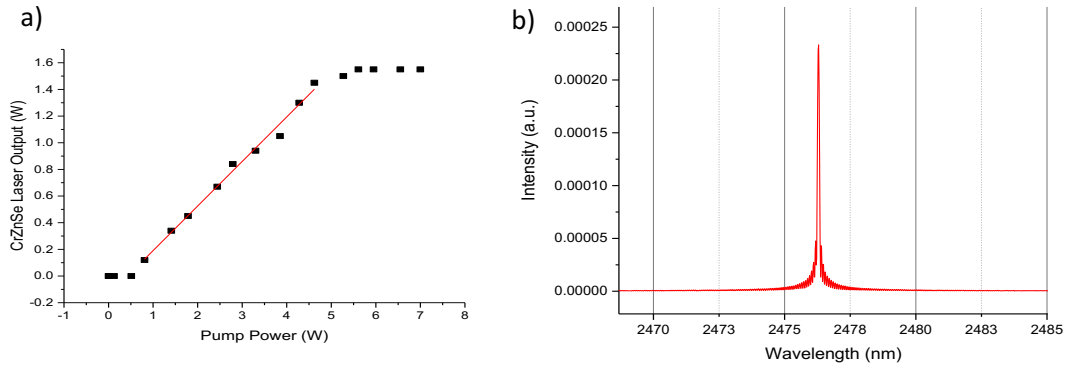

Figure. 18. (a) Power performance and (b) spectral emission from HIP CrZnSe in Z cavity.

The laser threshold occurs at ~ 0.43 W and has slope efficiency of ~ 33.4 % - the last 5 points are neglected in this calculation as thermal rollover occurs here. This is the expected result from the HIP treated material as we can see in Figure 18 (b) that the linewidth is very narrow and limited by the resolution of the OSA.

Modelocking Z-cavity Laser with SESAM

After establishing that the HIP treated CrZnSe was working as expected in the bulk Z-cavity an attempt at modelocking the laser was made. To do this, firstly the 80% OC was replaced with an one with a higher reflectivity of 97% at the lasing wavelength and the cavity length extended from ~ 40 cm for the CW work to ~ 82 cm. Using a high reflectivity OC and a longer cavity gives the cavity the best chance of producing the intracavity pulse energy required to pulse in the CW modelocked regime. The HR mirror is replaced in the cavity by a saturable absorber – in this case we used a SESAM fabricated by Del Mar Photonics and a 40 mm lens to focus onto it. The 40 mm lens was chosen as for smaller focal length lenses the spot may be focused too tightly which would result in damage, and for large focal length lenses, the spot may not be focus the beam sufficiently to saturate the SESAM. The key specifications of the Del Mar SESASM (SAM-2400-1-25) are the saturation fluence, relaxation time constant and modulation depth which are 90 $\mu J/cm^2$, 500 fs and 0.6% respectively. The output was then viewed on a 33 GHz Tektronix scope which was connected to a CMT detector (VIGO system PVM-10.6) which has a time constant of 1 ns. The crystal was pumped with a maximum of 3 W initially to protect the SESAM from damage. The detected output is shown in Figure 19. The average output power was 370 mW for 3 W of pump power. As we can see the laser is indeed pulsing with a repetition rate of ~ 180 MHz (this was also verified by viewing a peak in the RF spectrum here) which corresponds to the length of the cavity. However, the 'close-up' of the pulses shown in (b), shows that the pulses are quite long, of the order of 1-2 nm pulse width. The pump power was increased steadily and this pulsing behaviour was seen to be stable up to 4.5 W of pump power. At this level thermal issues caused a decrease in pulse stability, average power and overall beam quality. There was no observed obvious broadening of the spectral width and it remained narrow as shown in (c), this suggests that although there is some pulsing occurring in phase, this SESAM will not operate to produce ultrashort pulses for this cavity which is what we are interested in generating.

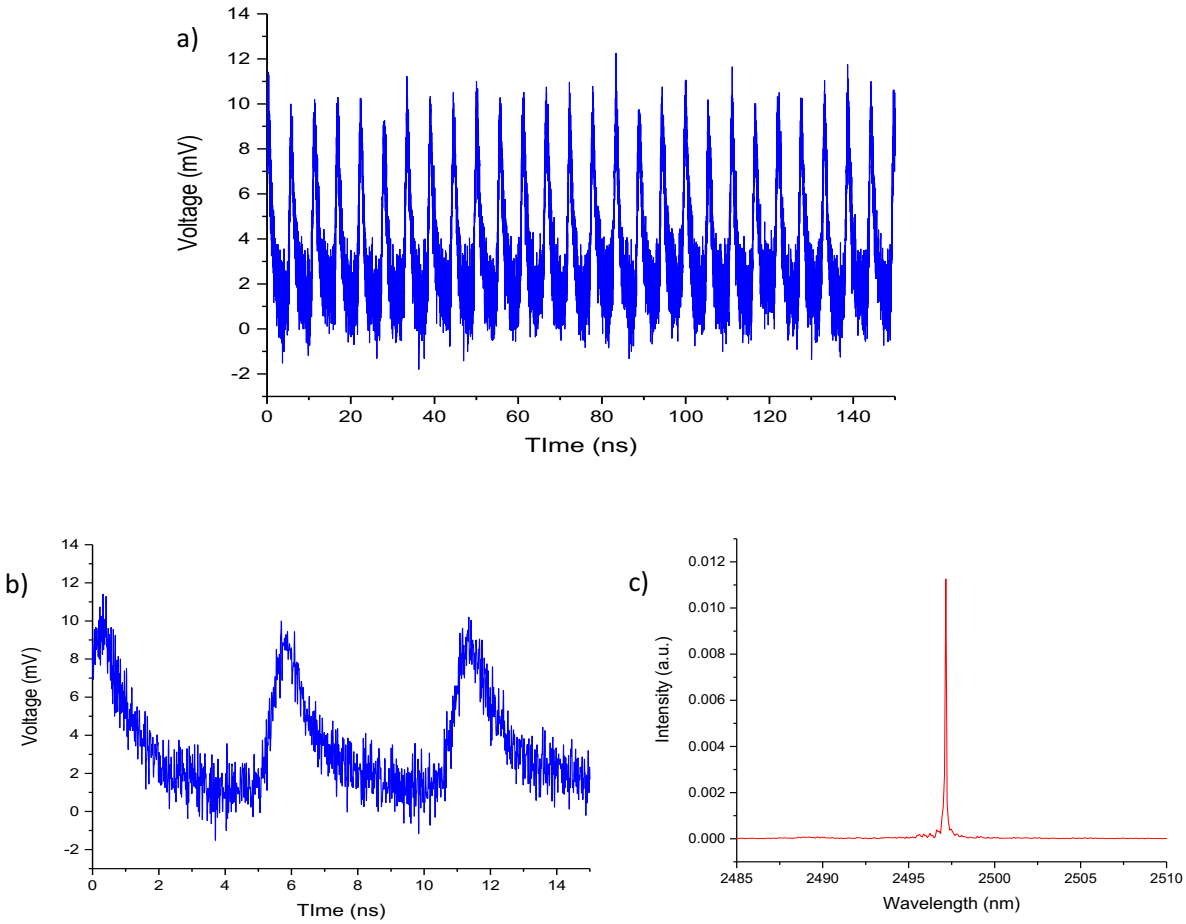

Figure 19. (a) Oscilloscope pulse trace and (b) is a close up of the pulses, (c) optical spectrum.

Future Work

The results are promising for modelocking HIP treated CrZnSe for the generation of short pulses. We believe that the choice of saturable will be paramount to doing this and so have 3 a major solutions to try. The first is simply to try a SESAM with better parameters which may be more suitable for this and also to include some dispersion compensation in the cavity. Initially, a new SESAM is going to be used to first establish pulsing ideally in the ps range, and then dispersion compensation to further shorten the pulses will be tried using methods such as; a prism pair, sapphire slab or other appropriate material. We will also attempt to cool the laser crystal and are at present in the process of designing a suitable Peltier cooling system. Another saturable asbsorber we plan to use is Graphene. Ajoy Kar has arranged with other collaborators to have graphene coated onto CaF_2 and Silicon substrates which will be inserted into the Z cavity as shown in Figure 20.

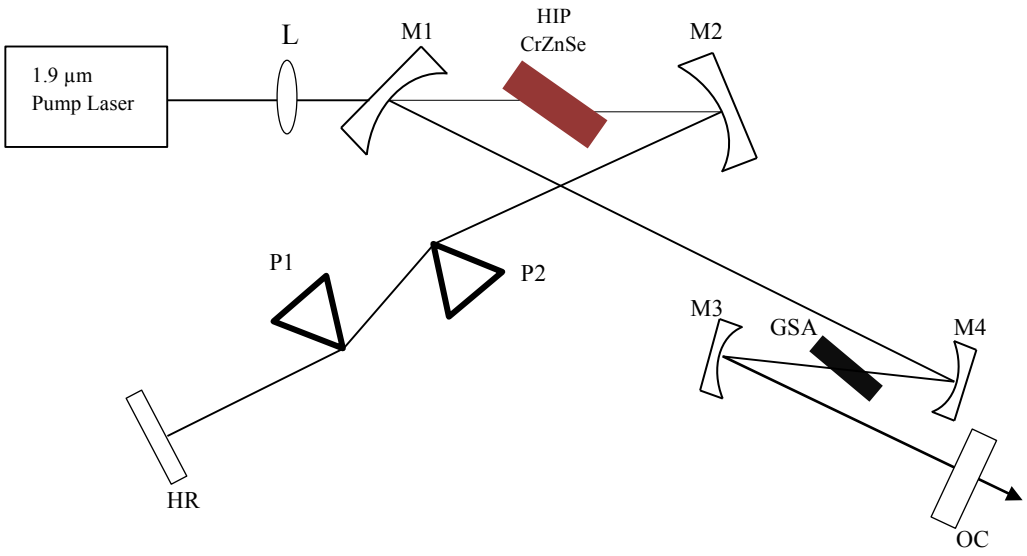

L: plano-convex focusing lens
M1, M2, M3 & M4: highly reflective plano-concave mirrors
HR: highly reflective plane mirror
OC: output coupler
P1 & P2: prisms for dispersion compensation (CaF_2), or could use sapphire slab we have or another material
GSA: Graphene saturbale absorber (Graphene coated onto silicon/CaF_2 substrate)

Figure 20. Cavity design for of HIP CrZnSe modelocked laser with Graphene SA.

We will also make attempts to modelock using Kerr Lens modelocking but research and experiments into this will begin after the above methods have been explored. In addition, research is continuing into the inscription of much lower loss waveguides in HIP treated material and these will be used for the development of a much higher repetition rate laser than will be possible with the current bulk z cavity set-up.

Summary

This year the work carried out in CrZnSe has focused on using the material when it has been treated by Hot Isostatic Pressing. The narrowing of the emission spectrum due to the treatment shows great potential for the purposes of modelocking for ultrashort pulses compared to the untreated material. We have built a CW HIP treated CrZnSe bulk laser here at HWU and the next stage of the work will focus on obtaining short pulses by trying a variety of modelocking techniques.

Publications and Forthcoming Publications

Title	Lead Author/Presenter & Description	Journal/Conference
Cr:ZnSe Guided Wave Lasers and Materials	**Gary Cook** Review of advances in the development of Cr:ZnSe waveguide lasers	**SPIE Photonics West 2017 SPIE LASE** San Francisco, CA, USA
Operation of Ho:YAG ultrafast laser inscribed waveguide lasers	**Sean McDaniel** Report of mid-IR multimode and single mode laser output from ULI waveguides in Ho:YAG	**Applied Optics, Vol. 56**(12), pages 3251-3256, April 2017.
5.9 GHz Q-Switched Mode-locked Mid-infrared Ho:YAG Waveguide Laser	**Fiona Thorburn** Report of Q-switched modelocked HoYAG waveguide laser	**Conference on Lasers and Electro-Optics(CLEO)** OSA Technical Digest (online) (Optical Society of America, 2017),paper SM1I.5.
5.9 GHz graphene based q-switched modelocked mid-infrared monolithic waveguide laser	**Fiona Thorburn** Full results of high rep. rate Q-switched modelocked HoYAG ULI waveguide laser	**Optics Express, Vol 25**(21), pages 26166-26174, October 2017.

References

1. T. Schweizer, "Rare-Earth-Doped Gallium Sulphide Glasses for Mid Infrared Fibre Lasers" University of Southampton, Faculty of Engineering, Science & Mathematics, Optoelectronics Research Centre, PhD Thesis, 1510T (2000).

2. L.C. Robinson, "Wave Transmission and Transmission Systems", Methods of Experimental Physics **10**, 82-156(1973).

3. A. P. Patel, and B. E. Knudsen, "Optimizing Use of the Holmium:YAG Laser for Surgical Management of Urinary Lithiasis," Current Urology Reports **15**, 397 (2014).

4. A. Sijan, "Development of military lasers for optical countermeasures in the mid-IR" Proc. SPIE 7483, 748304 (2009).

5. U. Keller, "Recent developments in compact ultrafast lasers," Nature **424**(6950), 831-838 (2003).

6. G. Sobon, J. Sotor, and K. M. Abramski, "Passive harmonic mode-locking in Er-doped fiber laser based on graphene saturable absorber with repetition rates scalable to 2.22 GHz," Appl. Phys. Lett. **100**(16), 161109 (2012).

7. G. T. Nogueira, B. Xu, Y. Coella, M. Dantus, and F. C. Cruz, "Broadband 2.12 GHz Ti:sapphire laser compressed to 5.9 femtoseconds using MIIPS," Optics Express **16**(14), 10033-10038 (2008).

8. R. R. Gattass, and E. Mazur, "Femtosecond laser micromachining in transparent materials," Nature Photonics **2**, 219-225 (2008).

9. R. R. Thomson, C. Leburn, and D. Reid, *Ultrafast Nonlinear Optics,* (Springer, 2003), Chap. 13.

10. R. Osellame, G. Cerullo, and R. Ramponi, *Femtosecond Laser Micromachining,* (Springer, 2012), Chaps 1 & 5.

11. D. Choudhury, J. R. Macdonald and A. K. Kar, "Ultrafast laser inscription: perspectives on future integrated applications," Laser and Photonics Reviews **8**(6), 827-846 (2014).

12. W. Nie, Y. Jia, J. R. Vázquez de Aldana, and F. Chen, "Efficient Second Harmonic Generation in 3D Nonlinear Optical-Lattice-Like Cladding Waveguide Splitters by Femtosecond Laser Inscription" Scientific Reports **6**, 22310 (2016).

13. Y. Jia, C. Cheng, J. R. Vázquez de Aldana, G. R. Castillo, B. Del Rosal Rabes, Y. Tan, D. Jaque and F. Chen, "Monolithic crystalline cladding microstructures for efficient light guiding and beam manipulation in passive and active regimes," Scientific Reports **4**, 5988 (2014).

14. M. Ganija, N. Simakov, A. Hemming, J. Haub, P. Veitch, and J. Munch, "Efficient, low threshold, cryogenic Ho:YAG laser," Optics Express **24**(11), 11569-11577 (2016).

15. B. Q. Yao, H. Li, X. Li, Y. Chen, X. Duan, S. Bai, H. Yang, Z. Cui, Y. Shen, and T. Dai, "An Actively Mode-locked Ho:YAG Solid-Laser Pumped by a Tm-Doped Fiber Laser," Chin. Phys. Lett. **33**(4), 044205 (2016).

16. J. W. Kim, J. I. Mackenzie, W. O. S. Bailey, L. Pearson, D. Y. Shen, Y. Yang and W. A. Clarkson, "Cryogenically-cooled Ho:YAG laser in-band pumped by a Tm fibre laser," in CLEO/Europe and EQEC 2009 Conference Digest, (Optical Society of America, 2009), paper CA10_5.

17. X. Duan, J. Yuan, Z. Cui, B. Yao, T. Dai, J. Li and Y. Pan, "Resonantly pumped actively mode-locked Ho:YAG ceramic laser at 2122.1 nm," Appl. Opt. **55**(8), 1953-1956 (2016).

18. II-VI Optical Systems Brochure, "Yttrium Aluminum Garnet Laser Materials" http://users.unimi.it/aqm/wp-content/uploads/YAGBrochure.pdf

19. J. E. Geusic, H. M . Macros, and L. G. Van Uitert, "Laser Oscillations in Nd-doped yttrium aluminium, yttrium gallium and gadolinium garnets," Appl. Phys. Lett **4**(10), 182 (1964).

20. P. Lacovara, H. K. Choi, C. A. Wang, R. L. Aggarwal, and T. Y. Fan, "Room-Temperature diode-pumped Yb:YAG laser," Optics Letters **16**(14), 1089-1091 (1991).

21. H. Eilers, W. M. Dennis, W. M. Yen, S. Kück, K. Peterman, G. Huber and W. Jia, "Performance of a Cr:YAG Laser," IEEE J. of Quant. Elec. **29**(9), 2508-2512 (1993).

22. A. Zajac, M. Skorczakowski, J. Swiderski, and P. Nyga, "Electrooptically Q-switched mid-infrared Er:YAG laser for medical applications," Optics Express **12**(21), 5125-5130 (2004).

23. N. Chang, D. J. Hosken, J. Munch, D. Ottaway, and P. J. Veitch, "Stable, Single Frequency Er:YAG Lasers at 1.6 μm," IEEE J. of Quant. Elec. **46**(7), 1039-1042 (2010).

24. M. E. Storm, D. J. Gettemy, N. P. Barnes, P. L. Cross, and M. R. Kokta, "Thulium YAG laser operation at 2.01 μm," Applied Optics **28**(3), 408-409 (1989).

25. R. Remski, and D. Smith, "Temperature Dependence of pulsed laser threshold in YAG:Er^{3+}, Tm^{3+}, Ho^{3+}," IEEE J. of Quan. Elec. **6**(11), 750-751 (1970).

26. M. E. Storm, "Laser characteristics of a Q-switched Ho:Tm:Cr:YAG," Applied Optics **27**(20), 4170-4172 (1988).

27. T. Y. Fan, G. Huber, R. L. Buyer, and P. Mitzscherlich, "Continuous-wave operation at 2.1 μm of a diode-laser-pumped, Tm-sensitized Ho:$Y_3Al_5O_{12}$ laser at 300 K," Optics Letters **12**(9), 678-679 (1987).

28. S. W. Henderson, and C. P. Hale, "Tunable single-longitudinal-mode diode laser pumped Tm:Ho:YAG laser," Applied Optics **29**(12), 1716-1718 (1990).

29. P. Liu, L. Jin, X. Liu, H. Huang, J. Zhang, D. Tang and D. Shen, "A Diode-Pumped Dual-Wavelength Tm,Ho: YAG Ceramic Laser," IEEE Photonics Journal **8**(5), 1504007 (2016).

30. Scientific Materials Corp. "Laser Materials Ho:YAG," http://www.scientificmaterials.com/products/ho-yag.php

31. S. McDaniel, F. Thorburn, A. Lancaster, R. Stites, G. Cook and A. Kar, "Operation of Ho:YAG ultrafast laser inscribed waveguide lasers," Applied Optics **56**(12), 3251-3256 (2017).

32. Y. Ren, G. Brown, R. Mary, G. Demetriou, D. Popa, F. Torrisi, A. C. Ferrari, F. Chen and A. K.Kar, "7.8-GHz Graphene-Based 2-μm Monolithic Waveguide Laser," IEEE J. of Sel. Topics in Quant. Elec. **21**(1), 1602106 (2015).

33. A. Okhrimchuk, V. Mezentsev, A. Shestakov, and I. Bennion, "Low loss depressed cladding waveguide inscribed in YAG:Nd single crystal by femtosecond laser pulses," Optics Express **20**(4), 3832-3843 (2012).

34. J. Zhang, K. F. Mak, S. Gröbmeyer, D. Bauer, D. Sutter, V. Pervak, F. Krausz, and O. Pronin, "Generation of 220 fs, 20 W pulses at 2 μm from Kerr-lens mode-locked Ho:YAG thin-disk oscillator," in *Conference on Lasers and Electro-Optics,* OSA Technical Digest (online) (Optical Society of America, 2017), paper SM1I.6.

35. Y. Wang, R. Lan, X. Mateos, J. Li, C. Hu, C. Li, S. Suomalaien, A. Härkönen, M. Guina, V. Petrov and U. Griebner, "Broadly tunable mode-locked Ho:YAG ceramic laser around 2.1 μm", Optics Express **24**(16), 18003-18012(2016).

36. C. Hönninger, R. Paschotta, F. Morier-Genoud, M. Moser and U. Keller, "Q-switching stability limits of continuous-wave passive modelocking," J. Opt. Soc. Am. B. **16**(1), 46-46 (1999).

37. Z. Sun, T. Hasan, and A. C. Ferrari, "Ultrafast lasers mode-locked by nanotubes and graphene," Physics E **44**(6), 1082-1091 (2012).

38. I. D. Jung, F. X. Kärtner, N. Matuschek, D. H. Sutter, F. Morier-Genoud, Z. Shi, V. Scheuer, M. Tilsch, T. Tschudi, and U. Keller, "Semiconductor saturable absorber mirrors supporting sub-10-fs pulses," Appl. Phys. B **65**, 137-150 (1997).

39. S. Husain, and R. G. Bedford, "Graphene saturable absorber for high power semiconductor disk laser mode-locking," Appl. Phys. Lett. **104**, 161107 (2014).

40. S. Yamashita, Y. Inoue, K. Hsu, T. Kotake, H. Yaguchi, D. Tanaka, M. Jablonski, and S. Y. Sey, "5-GHz Pulsed Fiber Fabry-Pérot Laser Mode-Locked Using Carbon Nanotubes," IEEE Photonics Tech. Lett. **17**(4), 750-725 (2005).

41. F. Thorburn, A. Lancaster, S. McDaniel, G. Cook, and A. K. Kar, "5.9 GHz Q-Switched Mode-locked Mid-infrared Ho:YAG Waveguide Laser," in *Conference on Lasers and Electro-Optics,* OSA Technical Digest (online) (Optical Society of America, 2017), paper SM1I.5.

42. F. Thorburn, A. Lancaster, S. McDaniel, G. Cook, and A. K. Kar, "5.9 GHz graphene based q-switched modelocked mid-infrared monolithic waveguide laser," Optics Express **25**(21), 26166-26174 (2017).

43. J. R. Macdonald, S. J. Beecher, P. A. Berry, G. Brown, K. L. Schelper and A. K. Kar, "Efficient mid-infrared Cr:ZnSe channel waveguide laser operating at 2486 nm," Optics Letters **38**(13), 2194-2196 (2013).

44. S. A. McDaniel, A Lancaster, J. W. Evans, A. K. Kar, and G Cook, "Power scaling of ultrafast laser inscribed waveguide lasers in chromium and iron doped zinc selenide," Optics Express **24**(4), 3502-3512 (2016).

45. A. Lancaster, J. R. Macdonald, S. J. Beecher, P. A. Berry, K. L. Schelper, and A. K. Kar, "Broadly tuneable Cr^{2+}:ZnSe channel waveguide laser," in Fibre Optics and Waveguides symposia, Photon 14, (2014).

46. R. W. Stities, S. A. McDaniel, J. O. Barnes, D. M Krien, J. H. Goldsmith, S. Ghua, and G. Cook, "Hot isostatic pressing of transition metal ions into chalcogenide laser host crystals," Optics Materials Express **6**(10), 3339-3353 (2016).